Kinetic Isotope Effects for Nonadiabatic Proton Transfer Reactions in a Polar Environment. 2. Comparison with an Electronically Diabatic Description

Philip M. Kiefer[†] **and James T. Hynes***[,†,‡]

Department of Chemistry and Biochemistry, University of Colorado, Boulder, Colorado 80309-0215, and Département de Chimie, CNRS UMR 8640 PASTEUR, Ecole Normale Supérieure, 24, rue Lhomond, 75231 Paris, France

Received: July 22, 2004; In Final Form: September 22, 2004

Kinetic isotope effects (KIEs) for proton transfer (PT) in a polar environment in the nonadiabatic, i.e., tunneling, regime was presented in the preceding paper (Kiefer, P. M.; Hynes, J. T, *J. Phys. Chem. A* **2004**, *108*, 0000). The present paper extends this work by comparing the electronically adiabatic (EAd) view of tunneling PT reactions of that paper with electronically diabatic (EDi) tunneling PT descriptions. Compared to the EAd PT description, the electronically diabatic character inherent in EDi PT produces smaller rate constants, larger KIE magnitudes with a smaller variation with reaction asymmetry, and a smaller activation energy difference $E_{AD} - E_{AH}$. Specifically, the EDi PT picture is characterized by a "nonadiabatic coupling" element that is smaller and less sensitive to both H-bond motion and proton vibrational excitation than those for EAd PT.

1. Introduction

In the preceding paper,[1] (hereafter called paper 1), a theoretical analysis for primary kinetic isotope effects (KIEs) was presented for proton transfer (PT) reactions in a polar environment, for the nonadiabatic "tunneling" PT regime derived from the basic formalism developed in ref 2. In this description, in which a solvent coordinate is the reaction coordinate, there is significant coupling between the proton donor-proton acceptor mode (H-bond mode, cf. eq 1.1 of paper 1[1]), also called a "promoting" or "gating" mode,[3−6] and the contribution of excited proton vibrational states to the total PT rate constants and KIEs is included.

In recent years there has been increased attention to tunneling PT reactions.[2−11] Coupling between H-bond dynamics and tunneling rates has, for example, been implicated in a variety of enzymatic[3−5,8] and nonenzymatic[7] reactions, where KIEs have been used to characterize the H-bond dynamics. These experimental results have often been analyzed using a picture for proton tunneling[9−11] which is related to that of refs 1 and 2; the reaction coordinate is also an environmental rearrangement, but there is the very important difference that weak electronic resonance coupling is assumed between the reactant and product equilibrium electronic configurations. We denote this alternate perspective as "electronically diabatic" (EDi) PT, such that the rate is proportional to the square of (a presumably small) electronic coupling. This strongly contrasts with the PT picture of refs 1 and 2, where the electronic structure adiabatically changes from reactant to product; i.e., there is a large electronic coupling, typical of bond-breaking and -making reactions. In the EAd picture, the electronic distribution changes continuously, whereas in EDi, the change is abrupt.

Arguments and evidence have been presented elsewhere[1,2,12] that the electronic adiabatic description is the one appropriate for PT (and H atom and hydride transfer) reactions, including tunneling reactions;[13] an electronically diabatic picture[9−11] is not appropriate.[15] (So-called proton-coupled electron transfer is a quite different reaction class, involving transfer of an electron over larger distances, where different considerations apply).[16−18] However, as noted above, the EDi PT picture has recently been applied to enzymatic and other systems,[4b,9d] and the differences in predictions of the electronically adiabatic and diabatic PT tunneling rates deserve clarification. One might expect that the rate constants in the two perspectives only differ by a constant (e.g., the square electronic coupling), but it will be shown that this is not the case. In particular, variation of the rate constants with, for example, temperature or reaction asymmetry leads to distinctly different behavior.

In the present paper, we provide a numerical comparison and discussion of the EDi PT perspective and the electronically adiabatic (EAd) PT picture described in paper 1,[1] focusing on the unimolecular situation of PT within a hydrogen-bonded (H-bonded) complex of an acid and base, e.g

$$AH\cdots B \rightleftharpoons A^{-}\cdots HB^{+} \qquad (1.1)$$

Specifically, the magnitude of rate constants, KIEs, and effective activation energies described in paper 1[1] for EAd PT are compared with those of the EDi PT picture. Section 2 presents the EDi PT formalism, including temperature and reaction asymmetry dependence. Section 3 compares and contrasts the KIE for both perspectives. Concluding remarks are offered in section 4.

2. Electronically Diabatic ProtonTunneling Formalism

In this section, the general rate constant formalism is presented for proton tunneling reactions, in which the electronic structure diabatically changes from reactant to product. Here we briefly review a limiting version of EDi PT[9−11] and then extend it to deal with contributions from excited proton states and H-bond dynamics. In particular, an expression for the slope in an Arrhenius plot is derived from this formalism, for later

* To whom correspondence should be sent. Telephone: (303) 492-6926. Fax: (303) 492-5894. E-mail: hynes@spot.colorado.edu.
† University of Colorado.
‡ Ecole Normale Supérieure.

10.1021/jp040498h CCC: $27.50
Published on Web 12/02/2004

use in the KIE temperature analysis of section 3c. The present derivation parallels the EAd PT formalism presented in paper 1,[1] and thus it facilitates a direct quantitative comparison between the two perspectives for PT.

2a. General Formalism. The rate expression for EDi PT is given by the electron-transfer rate constant expression with a Franck−Condon factor for proton reorganization.[9,11] The rate constant expression, including excitation in both the n_Rth reactant and n_Pth product proton vibrational modes, is a sum over all proton rearrangements

$$k = \frac{V_e^2}{\hbar}\sqrt{\frac{\pi}{\lambda RT}}\sum_{n_R} P_{n_R}\sum_{n_P}\exp(-\Delta\tilde{G}^{\ddagger}_{n_R,n_P}/RT)S_{n_R n_P} \quad (2.1)$$

where V_e is the electronic resonance-coupling between donor and acceptor, λ is the reorganization energy of the environment (an electronically diabatic reorganization energy[19]). The reaction barrier $\Delta\tilde{G}^{\ddagger}_{n_R,n_P}$ for each path is given by

$$\Delta\tilde{G}^{\ddagger}_{n_R,n_P} = \frac{(\lambda + \Delta G_{RXN} + \hbar\omega(n_P - n_R))^2}{4\lambda} \quad (2.2)$$

and P_{n_R} is the equilibrium thermal occupation probability of each reactant proton vibrational state. $S_{n_R n_P}$ is the square of the overlap of the reactant χ_{n_R} and product χ_{n_P} proton wave functions

$$S_{n_R n_P}(X) = |\langle\chi_{n_R}|\chi_{n_P}\rangle|^2 \quad (2.3)$$

which is explicitly dependent on the displacement X of the reactant and product wave functions, i.e., the tunneling distance. For two displaced harmonic oscillators of equal frequency ω, i.e., the frequency of the proton or deuteron vibrational mode, the overlap factor is analytically known[9]

$$S_{n_R n_P}(X) = n_R! n_P!\left(\frac{m\omega X^2}{2\hbar}\right)^{n_R - n_P} \times e^{-\Delta^2/2}\left[\sum_{k=0}^{n_P}\frac{\left(-\frac{m\omega X^2}{2\hbar}\right)^k}{k!(n_P-k)!(n_R-n_P+k)!}\right]^2 \quad (2.4)$$

The expression in eq 2.4 is for $n_R \geq n_P$, and is symmetric upon interchange of n_R and n_P (i.e., for $n_P \geq n_R$, n_R and n_P are interchanged in eq 2.4).

In the above, the proton donor−acceptor AB separation, i.e., the H-bond distance, which we denote by Q, (as in paper 1[1]), is held fixed. X is linearly related to the AB separation Q, as X plus the classical A−H and H−B equilibrium separations of the electronically diabatic reactant and product potentials: $Q = X + r_{AHeq} + r_{HBeq}$. In the EDi treatment, a *classical* average over H-bond motion is typically performed.[9,11] Here we use a harmonic mode for the H-bond vibrational mode with a frequency ω_Q, mass m_Q, and equilibrium AB separation Q_{eq}. An average over Q motion is equivalent to averaging over thermal fluctuations of the tunneling distance X, with frequency ω_Q, mass m_Q, and equilibrium distance $X_{eq} = Q_{eq} - r_{AHeq} - r_{HBeq}$.[21] Anharmonic modes can be used for both the proton and H-bond coordinates,[9] but do not significantly alter the physical picture or quantitative behavior for EDi PT. Since only $S_{n_R n_P}$ and V_e^2 depend on X, we consider the classical average over the H-bond motion of their product

$$\langle V_e^2 S_{n_R n_P}\rangle = \sqrt{\frac{m_Q\omega_Q^2}{2\pi RT}}\int_{-\infty}^{\infty} dX V_e^2 \times \exp[-m_Q\omega_Q^2(X - X_{eq})^2/2RT]|\langle\chi_{n_R}|\chi_{nP}\rangle|^2 \quad (2.5)$$

Here it is assumed that no H-bond mode reorganization occurs; i.e., the H-bond frequency and equilibrium separation do not significantly differ between reactant and product.[22]

The electronic resonance couplingV_e depends exponentially on the H-bond separation

$$V_e^2 = V_{eo}^2\exp[-2\alpha_e(X - X_{eq})] \quad (2.6)$$

where α_e is the inverse length scale of falloff of V_e, and is on the order of[20,23] 1 Å^{-1}. (Here we ignore any proton coordinate dependence of the electronic coupling.[23,24]) The X dependence in proton wave function overlap eq 2.4 can be expanded in the form

$$S_{n_R n_P} = e^{-(a_L X^2/2)}\sum_i c_{in_R n_P}\left(\frac{a_L X^2}{2}\right)^i \quad (2.7)$$

with coefficients $c_{in_R n_P}$,[25] so that the average in eq 2.5 is

$$\langle V_e^2 S_{n_R n_P}\rangle = V_{eo}^2\sum_i c_{in_R n_P}\sqrt{\frac{m_Q\omega_Q^2}{2\pi RT}}\int_{-\infty}^{\infty} dX\left(\frac{a_L X^2}{2}\right)^i e^{-(a_L X^2/2)} \times \exp[-2\alpha_e(X - X_{eq})]\exp[-m_Q\omega_Q^2(X - X_{eq})^2/2RT] \quad (2.8)$$

In the integral in eq 2.8

$$I_i = \sqrt{\frac{b}{2\pi}}\int_{-\infty}^{\infty} dX\left(\frac{a_L X^2}{2}\right)^i e^{-(a_L X^2/2)}e^{-2\alpha_e(X - X_{eq})}e^{-(b(X - X_{eq})^2/2)} \quad (2.9)$$

where we have introduced two quantities

$$a_L = m_L\omega_L/\hbar \quad (2.10)$$

$$b = m_Q\omega_Q^2/RT \quad (2.11)$$

the exponentials can be combined to give a more readily evaluated expression

$$I_i = \left(\frac{a_L}{2}\right)^i\sqrt{\frac{b}{2\pi}}e^{-(a_L b X_{eq}^2)/(2(a_L+b))}e^{(2\alpha_e(\alpha_e + X_{eq}a_L))/(a_L+b)} \times \int_{-\infty}^{\infty} dY\,(Y + B)^{2i}e^{-((a_L+b)/2)Y^2} \quad (2.12)$$

where $Y = X - bX_{eq}/(a_L + b)$ and $B = (bX_{eq} - 2\alpha_e)/(a_L + b)$. The definite integral in eq 2.12 has an analytical solution (detailed in ref 26), which we denote as

$$\int_{-\infty}^{\infty} dY\,(Y + B)^{2i}e^{-((a_L+b)/2)Y^2} = \gamma_i\sqrt{\frac{2\pi}{a_L + b}} \quad (2.13)$$

such that I_i is simply

$$I_i = \gamma_i\left(\frac{a_L}{2}\right)^i\sqrt{\frac{b}{a_L + b}}e^{-(a_L b X_{eq}^2)/(2(a_L+b))}e^{(2\alpha_e(\alpha_e + X_{eq}a_L))/(a_L+b)} \quad (2.14)$$

Combination of eqs 2.8 and 2.14 gives the final form of the average

$$\langle V_e^2 S_{n_R n_P}\rangle = V_{eo}^2\sqrt{\frac{b}{a_L+b}}\,e^{-(a_L b X_{eq}^2)/(2(a_L+b))}e^{(2\alpha_e(\alpha_e+X_{eq}a_L))/(a_L+b)}f_{n_R n_P} \quad (2.15)$$

where we have defined the extra contribution due to excited proton vibrational states

$$f_{n_R n_P} = \sum_i c_{i n_R n_P}\gamma_i\left(\frac{a_L}{2}\right)^i \quad (2.16)$$

The rate eq 2.1 is then

$$k_L = \frac{V_{eo}^2}{\hbar}\sqrt{\frac{\pi b}{(a_L+b)\lambda RT}}\times e^{-(a_L b X_{eq}^2)/(2(a_L+b))}e^{(2\alpha_e(\alpha_e+X_{eq}a_L))/(a_L+b)}\times \sum_{n_R}P_{n_R}\sum_{n_P}f_{n_R n_P}\exp(-\Delta\tilde{G}^{\ddagger}_{n_R,n_P}/RT) \quad (2.17)$$

Note that the evaluation of integrals and sums has been localized in f_{n_R,n_P}, which serves as a weight for each n_R to n_P transition. It proves useful to extract the n_R and n_P dependence of $\Delta G^{\ddagger}_{n_R,n_P}$, (cf. eq A.5 of paper 1[1])

$$\Delta\tilde{G}^{\ddagger}_{n_R,n_P} = \frac{(\Delta G_{RXN}+\lambda+(n_P-n_R)\hbar\omega)^2}{4\lambda} = \frac{(\Delta G_{RXN}+\lambda)^2}{4\lambda} + \frac{(n_P-n_R)\hbar\omega(2(\Delta G_{RXN}+\lambda)+(n_P-n_R)\hbar\omega)}{4\lambda} = \Delta\tilde{G}^{\ddagger}_{0,0}+\Delta\Delta\tilde{G}^{\ddagger}_{n_R,n_P} \quad (2.18)$$

such that the electronically diabatic PT rate is

$$k_L = \frac{V_{eo}^2}{\hbar}\tilde{\rho}_L\sqrt{\frac{\pi b}{(a_L+b)\lambda RT}}\times e^{-(a_L b X_{eq}^2)/(2(a_L+b))}e^{(2\alpha_e(\alpha_e+X_{eq}a_L))/(a_L+b)}e^{-\Delta\tilde{G}^{\ddagger}_{0,0}/RT} \quad (2.19)$$

The decomposition of the activation free energy reaction barrier in eq 2.18 into the ground state-to-ground state (0−0; the same notation used in paper 1[1]) free energy barrier—the first term—and the addition due to excited states—the second term—allows for a facile identification of the rate enhancement due to excited proton state reactions. Specifically, $\tilde{\rho}_L$ in eq 2.19 describes this rate enhancement

$$\tilde{\rho}_L(T) = \sum_{n_R}\sum_{n_P}f^{o}_{n_R n_P};\qquad f^{o}_{n_R n_P} = f_{n_R n_P}\exp[-\beta(n_R\hbar\omega+\Delta\Delta\tilde{G}^{\ddagger}_{n_R,n_P})] \quad (2.20)$$

(Here the assumption that $\hbar\omega/RT \gg 1$ is used to simplify $P_{n_R}\approx \exp(-\beta n_R\hbar\omega)$).

2b. Temperature Dependence. To obtain the temperature dependence of the rate expression eq 2.19, we wish to transform the rate constant into an Arrhenius form $k = A\exp(-\beta E_A)$, via a procedure analogous to that in Appendix B of paper 1.[1] The motivation here is application to experimental rate constant data measured in a limited T range centered around a value $T = T_o$ ($\beta = \beta_o$; cf. eq 3.12 of paper 1[1]), where the rate constant can be written as

$$k = k(T_o)\exp[-(\beta-\beta_o)E_A] \quad (2.21)$$

We seek an expression for the effective activation energy E_A. In the first step to derive this, the temperature dependence of the natural logarithm of eq 2.19 is expanded around $\beta = \beta_o$ (i.e., $\beta = \beta_o + \Delta\beta$), keeping only linear terms in $\Delta\beta$, (cf. eqs B.9−B.11 in paper 1[1]), giving for isotope L

$$\ln k_L = \ln k_{L00} - \Delta\beta\left(\frac{a_L^2 m_Q\omega_Q^2 X_{eq}^2}{2(a_L+b_o)^2}+\frac{2m_Q\omega_Q^2\alpha_e(\alpha_e+X_{eq}a_L)}{(a_L+b_o)^2}+\Delta G^{\ddagger}_{0,0}\right)+\ln\left[\sum_{n_R}\sum_{n_P}f^{o}_{n_R n_P}\exp[-\Delta\beta(n_R\hbar\omega+\Delta\Delta\tilde{G}^{\ddagger}_{n_R,n_P})]\right] \quad (2.22)$$

where k_{L00} is the ground-state to ground-state rate for $T = T_o$. Note that the first two terms in the coefficient for the $\Delta\beta$ term are due to the T dependence of b. (b_o in eq 2.22 is evaluated at $T = T_o$.)

Next, the logarithm of the summation in eq 2.22 is expanded in a Taylor series up to first order in $\Delta\beta$

$$\ln\left[\sum_{n_R}\sum_{n_P}f^{o}_{n_R n_P}\exp[-\Delta\beta(n_R\hbar\omega+\Delta\Delta\tilde{G}^{\ddagger}_{n_R,n_P})]\right] = \ln[\tilde{\rho}_L(T_o)]-\Delta\beta\langle\Delta\Delta\tilde{G}^{\ddagger}_{n_R,n_P}\rangle_L \quad (2.23)$$

where the extra effective activation energy due to excited proton states is

$$\langle\Delta\Delta\tilde{G}^{\ddagger}_{n_R,n_P}\rangle_L = \sum_{n_R}\sum_{n_P}f^{o}_{n_R n_P}[n_R\hbar\omega+\Delta\Delta\tilde{G}^{\ddagger}_{n_R,n_P}]\Big/\sum_{n_R}\sum_{n_P}f^{o}_{n_R n_P} \quad (2.24)$$

The isotope-dependent rate constant can then be written as

$$k_L(T) = k_{L00}(T_o)\tilde{\rho}_L(T_o)\exp\left[-\Delta\beta\left(\frac{a_L^2 m_Q\omega_Q^2 X_{eq}^2}{2(a_L+b_o)^2}+\frac{m_Q\omega_Q^2 2\alpha_e(\alpha_e+X_{eq}a_L)}{(a_L+b_o)^2}+\Delta G^{\ddagger}_{0,0}+\langle\Delta\Delta\tilde{G}^{\ddagger}_{n_R,n_P}\rangle_L\right)\right] \quad (2.25)$$

where the ground-state to ground-state rate k_{L00} for $T = T_o$ is

$$k_{L00}(T_o)\approx\frac{V_{eo}^2}{\hbar}\sqrt{\frac{\pi}{\lambda RT_o}}\sqrt{\frac{b_o}{a_L+b_o}}\times\exp\left[-\frac{1}{RT_o}\left(\frac{RT_o a_L b_o X_{eq}^2}{2(a_L+b_o)}-\frac{2\alpha_e RT_o(\alpha_e+X_{eq}a_L)}{a_L+b_o}+\Delta\tilde{G}^{\ddagger}_{0,0}\right)\right] \quad (2.26)$$

Equation 2.25 is now in the desired Arrhenius form with the activation energy identified as

$$E_{AL} = \frac{a_L^2 m_Q\omega_Q^2 X_{eq}^2}{2(a_L+b_o)^2}+\frac{m_Q\omega_Q^2 2\alpha_e(\alpha_e+X_{eq}a_L)}{(a_L+b_o)^2}+\Delta\tilde{G}^{\ddagger}_{0,0}+\langle\Delta\Delta\tilde{G}^{\ddagger}_{n_R,n_P}\rangle_L \quad (2.27)$$

which will be discussed in detail in section 3c in comparison with its EAd PT counterpart.

3. Comparison between Electronically Adiabatic and Diabatic Proton Transfer

The rate constants and KIEs of the EAd and EDi PT perspectives will now be compared numerically, using param-

eters for each perspective derived from the same PT system. For this purpose, we employ the model system for the acid−base PT used in our adiabatic PT studies:[14,23,27] a model H-bond system immersed in a dielectric continuum solvent, with a static dielectric constant $\epsilon_o = 80$. In particular, the electronic structure of the H-bonded complex is a mixture of electronically diabatic, valence bond (VB) states with diabatic dipole moments μ_R and μ_P for the reactant and product complexes. The vacuum nuclear (Morse) potentials for the AH and HB VB states have $\hbar\omega_P = 2900\ cm^{-1}$ and a classical proton minimum $q_o = 0.97$ Å. A large electronic resonance coupling, which mixes these reactant and product VB states, is exponential in the H-bond distance[2,9,11,20,23] (cf. eq 2.6)

$$V_e = V_{eo} \exp[-\alpha_e(Q - Q_{eq})] = V_{eo} \exp[-\alpha_e(X - X_{eq})] \quad (3.1)$$

with $V_{eo} = -19.2$ kcal/mol ($Q_{eq} = 2.95$ Å, $X_{eq} = 1.0$ Å) and $\alpha_e = 1.5\ Å^{-1}$ chosen for the present system.[14,20,23,27] We stress that this large electronic coupling value is appropriate for PT, as discussed in the Introduction, such that the reaction is in fact electronically adiabatic.[20] Finally, the H-bond equilibrium separation and frequency are chosen to ensure that PT is purely tunneling ($Q_{eq} = 2.95$ Å, $\hbar\omega_Q = 300\ cm^{-1}$, $m_Q = 15$ amu).

To further explore the differences between the two PT perspectives, two systems with differing reaction asymmetry and solvent reorganization energy will be used (system i, $\Delta G_{RXN} = 0$, $E_S = 19$ kcal/mol, and $\lambda = 22.4$ kcal/mol; system ii, $\Delta G_{RXN} = -5$ kcal/mol, $E_S = 9.7$ kcal/mol, and $\lambda = 12.3$ kcal/mol).[28] Here λ is the electronically diabatic reorganization energy introduced at eq 2.2, while E_S is a reorganization energy appropriate to the electronically adiabatic perspective in paper 1.[1] In each case, the relevant reorganization energy is that of the orientational polarization due to the change in dipole moment between reactant μ_R and product μ_P. The EAd reorganization energy E_S is defined, in a dielectric continuum solvent model, as[29] $E_S \approx (1/2)K(\mu_R - \mu_P)^2(\Delta c_P^2)^2$, where K contains the dependence on solvent polarity via the static and optical dielectric constants: $K = 2M_S(1/\epsilon_\infty - 1/\epsilon_o)$. M_S is a factor dependent on the structure of the H-bond complex. Δc_P^2 is the difference, between the reactant and product, in the contributions of the product valence bond state to the electronic structure. In these terms, the EDi λ is then defined as the zero electronic coupling limit[19] of E_S where $\Delta c_P^2 = 1$; $\lambda \approx (1/2)K(\mu_R - \mu_P)^2$. λ thus exceeds E_S due to a larger change in electronic structure between reactant and product inherent in an electronically diabatic approach.[14a]

This last statement about electronic structure is in fact a quite important and fundamental distinction between the two perspectives, and we devote some extended discussion to it here.Thus, in an electronically diabatic description for the example in eq 1.1, the charge distribution in the reactant state corresponds, at each value of the proton and H-bond coordinates q and Q to a limiting AH···B neutral pair structure, with no admixture from the product charge distribution, which would correspond to the limiting $A^-\cdots HB^+$ charge distribution. By contrast, in the electronically adiabatic perspective, the actual reactant charge distribution has some admixture of the limiting product charge distribution, and the actual product charge distribution has some admixture of the limiting reactant charge distribution. Thus, the electronically adiabatic reactant and product charge distributions are closer to each other than are those in the diabatic picture, i.e., the limiting structures referred to above. This key feature has a pervasive influence for the difference in the EAd and EDi

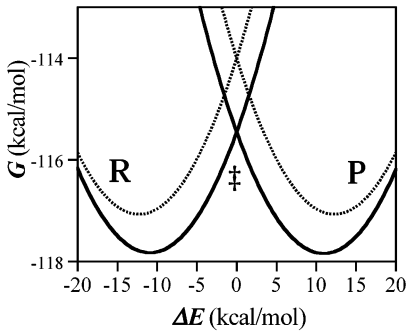

Figure 1. Ground- to ground- proton vibrational state free energy curves vs the solvent reaction coordinate for a continuum dielectric solvent model ($\epsilon_o = 80$, $M_S = 0.7$, $\mu_R = 0$, $\mu_P = 6$ D) for a symmetric PT reaction, $\Delta G_{RXN} = 0$, for both the EAd (solid line) and EDi (dashed line) PT perspectives. The reactant (R) and product (P) wells are indicated, as well as the transition state (‡) or curve crossing region. The H-bond mode is held fixed in this example at $Q = Q_{eq} = 2.95$ Å.

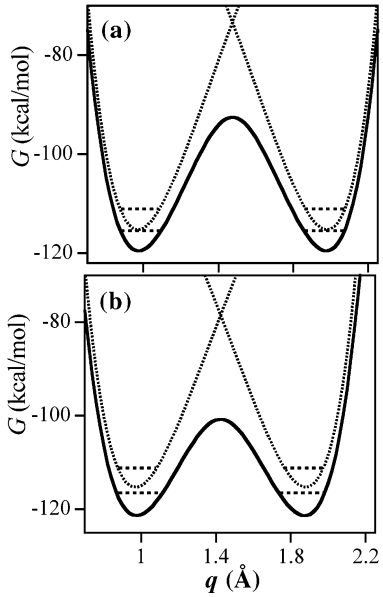

Figure 2. Electronically adiabatic (solid line) and diabatic (dotted lines) proton potentials at the transition state in the solvent coordinate: (a) $Q = Q_{eq} = 2.95$ Å; (b) $Q_{eq} = 2.85$ Å. Dashed lines indicate localized proton vibrational levels in the reactant and product. See the text for potential parameter details.

perspectives. For example, Figure 1 presents the free energy curves vs solvent coordinate for the proton ground state-to-ground state (0−0) transition for both perspectives using the same model system. The solvent coordinate ΔE is the energetic offset between the electronically diabatic states, which is modulated by the surrounding solvent.[30] The reactant and product well curvature and separation in this figure are larger for EDi PT compared with that for EAd PT, since the magnitude of both of these is greater for a larger difference in reactant-product charge distributions. The transition state (TS) in the solvent coordinate for each perspective is at the respective crossing between reactant and product wells, and at this TS the proton is able to tunnel, due to the resonance between the reactant and product proton vibrational levels. This basic feature is shared by the two perspectives, but Figure 2, which displays for each perspective the proton potentials at the fixed TS solvent coordinate value, shows that the ease of tunneling will differ considerably. The electronically diabatic proton wells have a larger curvature and are farther apart than their adiabatic counterparts, both of which are direct consequences of the larger electronic structure difference between reactant and product.[14,27]

Consequently, proton vibrational wave functions in the diabatic potentials will clearly be more localized than in the adiabatic wells. Hence, tunneling is more facile for EAd PT compared with EDi PT. This key aspect forms the basis of many aspects of our physical interpretation of the various results described in the remainder of this section.

In the numerical comparison of the two perspectives to follow, we will examine the EDi PT rates with the same large electronic coupling. This might appear inconsistent, i.e., in applying the EDi PT perspective with such coupling. However, this is the only way that the two formulations can be compared and corresponds, in our view, to the actual typical situation for literature applications of EDi PT theory. While one might think that the influence of the EDi assumption is limited to the appearance of a constant prefactor V_{eo}^2 in the rate, it will be seen below that this is not the case, a feature that can already be anticipated from Figures 1 and 2 and our discussion of them above.

3a. EAd and EDi Rates and KIE Magnitude. We begin the comparison with a brief presentation of each rate constant expression and any additional parameters that enter each. For EAd PT, we use the rate constant from paper 1[1] for the moderate to high T range ($\hbar\omega_Q/RT \sim 1$ and $\hbar\omega_Q/RT < 1$), where explicit expressions for the T dependence have been derived, (cf. eqs 3.13 and 3.14 of paper 1[1])

$$k_{L,EAd} = \frac{C_{eqL}^2(Q_{eq})}{\hbar}\rho_L\sqrt{\frac{\pi}{(E_S + \tilde{E}_{\alpha L})RT}} \times \exp\left(2\frac{E_{\alpha L}}{\hbar\omega_Q}\coth((^1/_2)\beta\hbar\omega_Q)\right)\exp\left[-\frac{\Delta G^{\ddagger}_{L0,0}}{RT}\right] \quad (3.2)$$

The reaction free energy barrier in eq 3.2 is that for the ground state-to-ground-state transition (cf. eq 2.25 in paper 1[1])

$$\Delta G^{\ddagger}_{L0,0} = \frac{(\Delta G_{RXN} + E_S + E_{\alpha L})^2}{4(E_S + \tilde{E}_{\alpha L})} \quad (3.3)$$

and the factor ρ_L contains the contributions to the rate from excited proton vibrational state transitions (cf. eq 3.3 in paper 1[1]). $E_{\alpha L}$ is a quantum energy term associated with the tunneling probability's variation with the Q vibrational coordinate (cf. eq 2.7 of paper 1[1])

$$E_{\alpha L} = \hbar^2\alpha_L^2/2m_Q; \quad \tilde{E}_{\alpha L} = E_{\alpha L}(^1/_2)\beta\hbar\omega_Q\coth((^1/_2)\beta\hbar\omega_Q) \quad (3.4)$$

The factors α_L and C_{eqL} are related to the proton (not the electronic) coupling $C_L(Q)$ governing the tunneling probability (cf. eq 2.4 in paper 1[1]), which is exponential in the H-bond separation Q:

$$C_L(Q) = C_{eqL}\exp[-\alpha_L(Q - Q_{eq})]; \quad \langle C_L^2\rangle = C_L^2(Q_{eq})\exp[2E_{\alpha L}\coth(\beta\hbar\omega_Q/2)/\hbar\omega_Q] \quad (3.5)$$

where we have also written out the thermal average of the square of the coupling, to which the rate constant is proportional. C_{eqL} is the value of the proton coupling for the 0−0 proton transition, evaluated at the equilibrium value Q_{eq} for the H-bond coordinate, while α_L is the spatial decay rate of the proton coupling with respect to Q, and contains an important isotope mass dependence $\alpha_L \propto \sqrt{m_L}$ ($E_{\alpha L} \propto m_L$; cf. section 2b in paper 1[1]). These factors are determined using a model for the proton potential[14] that is derived from mixing two displaced Morse potentials with the electronic coupling: $\alpha_H = 29$ Å^{-1} and $\alpha_D = 41$ Å^{-1}, values which are taken to be independent of transition (as determined from numerical results). C_{eqL} is determined via eq 2.21 in paper 1,[1] where the proton coordinate frequencies in the reactant and product wells and at the proton barrier top are $\omega_R = \omega_P = 2800$ cm^{-1}, $\omega^{\ddagger} = 2200$ cm^{-1}, with the proton barrier $V^{\ddagger} = 27$ kcal/mol at $Q = Q_{eq}$.

TABLE 1: Rate Characteristics Comparisons for EAd and EDi Perspectives

	k_H (s^{-1})	k_D (s^{-1})	KIE	E_{AH} (kcal/mol)	$E_{AD} - E_{AH}$ (kcal/mol)
EAd PT (i)	1.98E+04	2.54E+03	7.8	9.4	7.3
EAd PT (ii)	3.56E+07	6.47E+06	5.5	5.5	7.2
EDi PT (i)	0.215	1.55E−04	1386	11.1	3.7
EDi PT (ii)	57	0.485	1193	6.7	3.7

The EDi PT rate constant including transfer between reactant and product excited proton states is (cf. eq 2.19)

$$k_{L,EDi} \approx \frac{V_{eo}^2}{\hbar}\tilde{\rho}_L\sqrt{\frac{\pi}{\lambda RT}}\sqrt{\frac{b}{a_L + b}} \times \exp\left[-\frac{a_L b X_{eq}^2}{2(a_L + b)} + \frac{2\alpha_e(\alpha_e + X_{eq}a_L)}{a_L + b}\right]\exp\left[-\frac{\Delta\tilde{G}^{\ddagger}_{00}}{RT}\right] \quad (3.6)$$

With the formalism for each perspective in hand, the numerical results for eqs 3.2 and 3.6 can be compared. Table 1 displays the rate constants, the KIE k_H/k_D, and the effective activation energies E_{AL} for each perspective for both systems (i) and (ii). The E_{AL} values were obtained numerically from the slope of a ln k vs $1/RT$ plot ($T = 275-325$ K). Most evident from Table 1 are the drastic differences in rate constant and KIE magnitudes, with larger rates for EAd PT and a larger KIE for EDi PT. In addition, E_{AH} and E_{AD} are similar for EAd and EDi PT, but the difference $E_{AD} - E_{AH}$ is ∼2-fold larger for EAd PT. We first focus on the distinct differences in rate constant and KIE magnitudes, with a discussion of the reaction asymmetry dependence in section 3b, while a discussion of the temperature dependence and isotopic difference in effective activation energies is reserved for section 3c.

The rate expressions eqs 3.2 and 3.6 are qualitatively similar, in a general way, with a solvent activation free energy, certain prefactor terms, including the excited proton vibrational state factors, and what we term "nonadiabatic coupling" elements now to be made precise. We focus on these last factors for comparison since the first two will turn out to be relatively similar in magnitude. For quantitative comparison, portions of eqs 3.2 and 3.6 are thus extracted to emphasize the thermal average of the nonadiabatic coupling elements over H-bond motion

$$k_{L,EDi} \propto \langle V_e^2 S_{00}\rangle = V_{eo}^2\sqrt{\frac{b}{a_L + b}}\exp\left[-\frac{a_L b X_{eq}^2}{2(a_L + b)} + \frac{2\alpha_e(\alpha_e + X_{eq}a_L)}{a_L + b}\right] = K_{L,EDi} \quad (3.7)$$

$$k_{L,EAd} \propto \langle C_L^2\rangle = C_{eqL}^2\exp(2E_{\alpha L}\coth((^1/_2)\beta\hbar\omega_Q)/\hbar\omega_Q) = K_{L,EAd} \quad (3.8)$$

We first establish that these coupling factors $K_{L,EAd}$ and $K_{L,EADi}$ contain a large portion of the differences in the two perspectives for the rate constant and KIE magnitudes. First, the ratio of $K_{H,EAd}$ and $K_{H,EDi}$, is 54628, which is similar in magnitude to

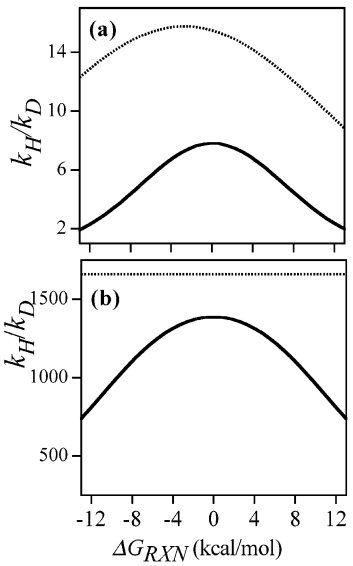

Figure 3. Kinetic isotope effect k_H/k_D vs the reaction asymmetry ΔG_{RXN} for system i for EAd PT(a) and EDi PT (b). Both the 0−0 proton transition KIE (dotted lines) and total rate KIE (solid lines) are displayed.

the ratio of the rate constant k_H for the two perspectives, $k_{H,EAd}/k_{H,EDi} = 92093$ for system i. Furthermore, the H vs D ratio for $K_{L,EDi}$ in eq 3.7, $K_{H,EDi}/K_{D,EDi} = 1659$, is quantitatively similar to e.g. $KIE_{EDi} = 1386$ for system (i). Finally, the H vs D ratio for $K_{L,EAd}$ in eq 3.8, $K_{H,EAd}/K_{D,EAd} = 5.6$, is also quantitatively similar to the corresponding KIE, $KIE_{EAd} = 7.8$ for system i, which is much smaller than KIE_{EDi}. Clearly, the respective nonadiabatic coupling factors K in eqs 3.7 and 3.8 quantitatively capture most of the drastic rate constant and KIE disparities between the two perspectives.

The disparity in the rate constant k_H pointed out above in which the EAd rate far exceeds the EDi rate arises despite the presence of a large electronic coupling element in the EDi eq 3.7 (which, with all other things being equal, would give a large prefactor for the EDi rate compared to the EAd rate). Furthermore, this factor cancels out in KIE_{EDi}, and so cannot be responsible for the very large discrepancy in the KIEs for the two perspectives. The primary reason for the large differences in the two perspectives lies in the proton contribution to the coupling prefactors; for $K_{L,EDi}$, this contribution is a Franck−Condon overlap of proton wave functions localized in reactant and product electronically diabatic potentials, which contrasts with $K_{L,EAd}$ which derives from a proton resonance vibrational splitting on an electronically adiabatic surface. As we have already anticipated in the introduction of this Section in connection with Figure 2, the overlap of proton wave functions localized in the R and P proton wells will be larger for the electronically adiabatic surface than for the diabatic one, and tunneling will be easier in the adiabatic perspective. Because of this same feature, the greater difficulty in tunneling for the diabatic perspective, with its larger separation between the R and P wells, makes the rate constant more sensitive to isotopic substitution of D for H, resulting in a larger KIE.

3b. Kinetic Isotope Variation with Reaction Asymmetry. To further expand on the difference in KIE magnitude between the two perspectives, we now consider the KIE variation with reaction asymmetry. Figure 3 displays the KIE vs ΔG_{RXN} behavior for system i in both perspectives. Also shown is the KIE behavior including only the ground proton level 0−0 transition contributions to the rates. As discussed in paper 1,[1] the 0−0 KIE behavior for EAd PT falls off with increased reaction asymmetry due to the increased probability of excitations in the H-bond mode with increasing reaction asymmetry[31]—this is in stark contrast to the KIE behavior with EDi PT, where the 0−0 KIE is constant. For the total EAd rate, an additional falloff occurs due to the increased contributions from excited proton vibrational states with increasing reaction asymmetry (the ρ_L factor in eq 3.2); Figure 3 shows that the KIE falloff for EAd PT is larger and of a somewhat different shape than for EDi PT.

We can expand on these observations by examining the KIE expression for EDi PT, H vs D, derived from the isotopic ratio of eq 3.6

$$\frac{k_{H,EDi}}{k_{D,EDi}} \approx \frac{\tilde{\rho}_H}{\tilde{\rho}_D}\sqrt{\frac{a_D+b}{a_H+b}}\exp\left[-\frac{bX_{eq}^{\,2}}{2}\left(\frac{a_H}{a_H+b}-\frac{a_D}{a_D+b}\right)+2\alpha_e\left(\frac{\alpha_e+a_HX_{eq}}{a_H+b}-\frac{\alpha_e+a_DX_{eq}}{a_D+b}\right)\right] \quad (3.9)$$

in which the isotope-dependent quantities have been indicated. The ratio $\tilde{\rho}_H/\tilde{\rho}_D$ of rate enhancements explicitly carries the dependence on excited states, while the exponential terms are due to the classical thermal averaging of the H-bond mode over the H-bond separation and electronic coupling. The KIE reaction asymmetry dependence here arises solely from the enhancement ratio $\tilde{\rho}_H/\tilde{\rho}_D$, and it is only when excited proton vibrational levels are added that the KIE falls off with increased reaction asymmetry, whereas for the EAd PT of paper 1,[1] excitation of the H-bond vibrations contribute as well; this is the reason for the strong qualitative difference of the 0−0 contribution to the KIE in Figure 3. As noted earlier, the EDi perspective treatments describe the H-bond classically,[9−11] (although this is an issue logically distinct from the assumption of weak electronic coupling), while the EAd perspective has explicitly treated the H-bond mode quantum mechanically, with the consequence that the rate constant eq 3.2 (cf. eqs 2.10 and 2.11 in paper 1[1]) explicitly contains an isotope-dependent quantum localization term $E_{\alpha L}$ into the state-to-state free energy relationship (FER) connecting the reaction free energy barrier and the reaction asymmetry. This contrasts with the state -to-state FER for EDi PT which is isotope-*independent* (cf. eq 2.2). The lack of quantum H-bond treatment by EDi PT gives a decreased KIE variation with reaction asymmetry, only a factor of ∼2 in Figure 3, compared to the factor of ∼4 effect for EAd PT.[22]

3c. Effective Activation Energies. We next examine the isotope-dependent temperature dependence of the rate constants focusing on the effective activation energies E_{AL} for both perspectives. We first deal with the general features for both isotopes, for which Table 1 shows that E_{AH} is smaller by about 1−1.5 kcal/mol for the EAd description, depending on the system. We then focus on the differences between isotopes, and in particular, on the ∼2-fold difference in Table 1 for $E_{AD} - E_{AH}$ between the two perspectives (which is the same for the two systems).

3c.1. Individual Effective Activation Energies and their Components. The effective activation energy for the EAd rate eq 3.2 is (cf. eq 3.14 in paper 1[1])

$$E_{AL,EAd} = E_{AQ,EAd} + \Delta G^{\ddagger}_{L0,0} + \langle \Delta\Delta G^{\ddagger}_{n_R,n_P}\rangle_L \quad (3.10)$$

where the first term is the activation energy contribution arising from the thermal average of the square proton coupling $\langle C^2\rangle$ over the H-bond vibration (cf. eq 2.16 of paper 1[1]), reflecting the T dependence of the Q vibration

$$E_{AQ,EAd} = E_{\alpha L}[\coth^2(\beta_o \hbar\omega_Q/2) - 1] \quad (3.11)$$

The second term is the 0−0 activation free energy barrier $\Delta G^{\ddagger}_{L0,0}$, and the third term is the activation energy free contribution from excited proton states, arising from the temperature dependence of $\rho_L(T)$.

The effective activation energy for EDi PT has a somewhat analogous decomposition (cf. eq 2.27)

$$E_{AL,EDi} = E_{AQ,EDi} + E_{AV} + \Delta\tilde{G}^{\ddagger}_{0,0} + \langle\Delta\Delta\tilde{G}^{\ddagger}_{n_R,n_P}\rangle_L \quad (3.12)$$

in which $E_{AQ,EDi}$ is due to the impact of the thermal excitation of Q on the overlap of proton reactant and product wave functions, while E_{AV}, which has no direct analogue in the EAd picture, arises from the Q dependence of the electronic coupling prefactor in eq 3.2:

$$E_{AQ,EDi} = \frac{a_L{}^2 m_Q \omega_Q{}^2 X_{eq}{}^2}{2(a_L + b_o)^2}; E_{AV} = \frac{m_Q \omega_Q{}^2 2\alpha_e(\alpha_e + X_{eq} a_L)}{(a_L + b_o)^2} \quad (3.13)$$

The third term in eq 3.12 is the solvent free energy barrier contribution $\Delta\tilde{G}^{\ddagger}_{0,0}$ from the 0−0 transition, while the fourth term gives the corresponding contribution involving excited proton states, arising from the temperature dependence of $\tilde{\rho}_L(T)$ (see the developments around eq 2.24).

Tables 2 and 3 display the calculated E_{AL}s from eqs 3.10 and 3.12 for the symmetric (i) and asymmetric (ii) systems, respectively. Included in each table are the individual contributions from each component; the ordering is as in eqs 3.10 and 3.12, except that there is no analogue for EAd PT of electronic coupling term E_{AV}**.** Notice that the E_{AL} values in Tables 2 and 3 obtained from our analytical treatment are close to those in Table 1, obtained numerically, supporting the validity of the analysis. We now analyze E_{AL} in more detail, postponing most discussion of the isotopic differences until section 3c.2.

In both perspectives and for each system, a dominant contribution to E_{AL} comes from the effective activation energy E_{AQ}. The E_{AQ} term for both EAd and EDi PT primarily corresponds to the T dependence of the Ks in eqs 3.7 and 3.8. In particular, the connection of the Ks to thermal averaged nonadiabatic coupling elements (eqs 3.7 and 3.8) depicts E_{AQ} as a thermal activation energy contribution due to the coupling between proton wave function overlap and thermal excitation of the H-bond mode. Furthermore, E_{AQ} is system-independent (i.e., the same for i and ii), reflecting the K factors' lack of dependence on reaction asymmetry and reorganization energy, i.e., only dependent on the H-bond mode characteristics. The electronic coupling contribution E_{AV} adds to the T dependence of $K_{L,EDi}$, but the amount is minimal due to the relatively weak Q dependence of the electronic coupling, related to the slow Q variation of the overlap of slowly decaying R and P electronic wave functions; accordingly, E_{AV} is ignored in our further discussions. Finally, E_{AQ} for the H isotope is ∼1 kcal/mol smaller in the EAd description than in EDi, but there is almost no difference for the D isotope; this will play a role in our section 3c.2 discussion.

The 0−0 reaction free energy barrier $\Delta G^{\ddagger}_{L0,0}$ also significantly contributes to E_{AL}, and here the reorganization energy and reaction asymmetry are critical components (cf. eqs 2.2 and 3.3). These isotope-independent factors dominate in each perspective; $\Delta G^{\ddagger}_{L0,0}$ is, however, slightly isotope-dependent in EAd PT, due to a small contribution by the isotope-dependent $E_{\alpha L}$ (see eq 3.4). The factor of 5 decrease in $\Delta G^{\ddagger}_{L0,0}$ going from i to ii reflects a decrease in reorganization energy (both E_S and λ) and an increase in reaction asymmetry. The fact that for each system $\Delta G^{\ddagger}_{L0,0}$ is similar in magnitude for both perspectives (differences of 0.5 kcal/mol or less) reflects the comparable magnitudes of reorganization energy for EDi and EAd PT, such that $\Delta G^{\ddagger}_{L0,0}$ is not a source of any significant difference between the EAd and EDi descriptions.

TABLE 2: Effective Activation Energy Components for System i (Energies in kcal/mol)

	E_{AL}	E_{AQ}	E_{AV}	$\Delta G^{\ddagger}_{L0,0}$	$\langle\Delta\Delta G^{\ddagger}_{n_R,n_P}\rangle_L$	ρ_L
EAd PT H	9.9	4.38	NA	5.31	0.22	1.04
EAd PT D	17.4	8.76	NA	5.87	2.83	2.07
EDi PT H	11.6	5.52	0.39	5.60	0.06	1.01
EDi PT D	15.4	8.67	0.43	5.60	0.66	1.21

TABLE 3: Effective Activation Energy Components for System ii (Energies in kcal/mol)

	E_{AL}	E_{AQ}	E_{AV}	$\Delta G^{\ddagger}_{L0,0}$	$\langle\Delta\Delta G^{\ddagger}_{n_R,n_P}\rangle_L$	ρ_L
EAd PT H	5.9	4.38	NA	1.06	0.48	1.15
EAd PT D	13.5	8.76	NA	1.59	3.18	3.15
EDi PT H	7.1	5.52	0.39	1.08	0.12	1.03
EDi PT D	11.1	8.67	0.43	1.08	0.86	1.44

In each description, the additional excitation free energy due to transitions other than the 0−0 transition $\langle\Delta\Delta G^{\ddagger}_{n_R,n_P}\rangle$ is relatively small for the H isotope, predominantly due to the dominant though not always exclusive contribution of the 0−0 transition; i.e., ρ_L is near 1**.** The contribution for the D isotope is however nonnegligible in the EAd description, while it remains small in the EDi characterization. This will be important in section 3c.2. Finally, as discussed in section 3b, ρ_L (and $\tilde{\rho}_L$) will increase with increasing reaction asymmetry, an effect visible in the increased $\langle\Delta\Delta G^{\ddagger}_{n_R,n_P}\rangle$ contribution going from i to ii, but not changing the patterns for H and D just described.

3c.2. Effective Activation Energy Isotope Dependence. We now compare in the two perspectives the E_{AL} isotopic difference $E_{AD} - E_{AH}$ governing the temperature dependence of the kinetic isotope effect k_H/k_D. From Table 1, this difference is twice as large, and ∼3.5 kcal/mol larger, for the EAd treatment than that for EDi, for each of the model systems. This ∼3.5 kcal/mol excess for EAd PT can be further broken down via Tables 2 and 3: ∼1 kcal/mol in $E_{AQ,D} - E_{AQ,H}$, ∼0.5 kcal/mol in $\Delta G^{\ddagger}_{D0,0} - \Delta G^{\ddagger}_{H0,0}$, and ∼2 kcal/mol in $\langle\Delta\Delta G^{\ddagger}_{n_R,n_P}\rangle_D - \langle\Delta\Delta G^{\ddagger}_{n_R,n_P}\rangle_H$. As mentioned above, the $\Delta G^{\ddagger}_{D0,0} - \Delta G^{\ddagger}_{H0,0}$ contribution, only present for EAd PT, comes from an isotope-dependent free energy relationship eq 3.3, via the dependence on $E_{\alpha L} \propto m_L$, so that $E_{\alpha D} \sim 2E_{\alpha H}$. This contribution is, however, small because $E_{\alpha L}$ is smaller than the reorganization energy E_S in eq 3.3. The more significantly contributing isotopic differences of $\langle\Delta\Delta G^{\ddagger}_{n_R,n_P}\rangle_L$ and E_{AQ} are now discussed.

The next important ingredient in $E_{AD} - E_{AH}$ is the contribution from excited proton states $\langle\Delta\Delta G^{\ddagger}_{n_R,n_P}\rangle_L$, which is the key ingredient in the T dependence of ρ_L and $\tilde{\rho}_L$

$$\rho_L(T) = \rho_L(T_o)\exp\left[-\langle\Delta\Delta G^{\ddagger}_{n_R,n_P}\rangle_L\left(\frac{1}{RT} - \frac{1}{RT_o}\right)\right] \quad (3.14)$$

(Note that ρ_L in eq 3.14 generally applies to both ρ_L and $\tilde{\rho}_L$, which will also apply in the following discussion.) We have already seen in section 3b that ρ_L increases with reaction asymmetry because the increased "nonadiabatic coupling" (proton wave function overlap) that accompanies excited proton and H-bond vibrational states increases with reaction asymmetry. Increasing the temperature also increases the thermal population

of proton/deuteron excited states, and this increase is larger for the heavier isotope D; thermal excitation is more facile for D compared to H since $\hbar\omega_H > \hbar\omega_D$. This increased D excitation effect has more impact for EAd than for EDi, primarily due to a smaller $\hbar\omega_D$ value for EAd than for EDi PT.

The difference $E_{AQ,D} - E_{AQ,H}$, is the largest contribution for $E_{AD} - E_{AH}$ for both perspectives, and because it is determined by the H-bond mode properties, we now elaborate on the origin of this difference. As mentioned above, E_{AQ} is predominantly due to the temperature dependence of the Q thermal excitation effects contained in the nonadiabatic coupling elements Ks eqs 3.7 and 3.8. The T dependence of the Ks can be viewed in terms of effective activation energies, i.e.

$$K_L(T) = K_L(T_o)\exp\left[-E_{AQ,L}\left(\frac{1}{RT} - \frac{1}{RT_o}\right)\right] \quad (3.15)$$

where the effective activation energies $E_{AQ,L}$s are given by eqs 3.11 and 3.13. (Here the contribution of the electronic coupling variation with Q to $K_{L,EDi}$ has been ignored.) Before proceeding, it will be useful to write out the $E_{AQ,L}$s using eqs 3.7, 3.8, and 3.15. Furthermore, to compare the $E_{AQ,L}$s and their isotope dependence using an equivalent description of the H-bond mode, we focus on the classical Q limit. In this limit, the adiabatic PT activation energy contribution $E_{AQ,EAd}$, is[32]

$$E_{AQ,EAd} = 4\frac{\hbar^2\alpha_{EAdL}{}^2}{2m_Q}\left(\frac{RT_o}{\hbar\omega_Q}\right)^2 = RT_o 2\alpha_{EAdL}{}^2\langle\delta Q^2\rangle_{cl} \quad (3.16)$$

where the last line is written to emphasize the dependence on $\alpha_{EAdL} \equiv \alpha_L$, the coupling between proton wave function overlap and Q (cf. eq 3.5), and the thermal classical average square fluctuation of Q

$$\langle\delta Q^2\rangle_{cl} = \frac{RT_o}{m_Q\omega_Q{}^2} \quad (3.17)$$

(We have introduced in this subsection only the notation $\alpha_{EAdL} \equiv \alpha_L$ in order to make clear which quantities are being compared in the two perspectives.) For the EDi case, with the neglect of the small electronic coupling contribution in the exponent of K in eq 3.7, we have

$$K_{L,EDi} \propto \langle S_{00}\rangle = \sqrt{\frac{2\langle\delta q^2\rangle_L}{\langle\delta Q^2\rangle_{cl} + 2\langle\delta q^2\rangle_L}}\exp\left[-(1/2)\frac{X_{eq}{}^2}{\langle\delta Q^2\rangle_{cl} + 2\langle\delta q^2\rangle_L}\right] \quad (3.18)$$

such that the corresponding activation energy defined from eq 3.15 is

$$E_{AQ,EDi} = (1/2)RT_o\frac{\langle\delta Q^2\rangle_{cl}X_{eq}{}^2}{(\langle\delta Q^2\rangle_{cl} + 2\langle\delta q^2\rangle_L)^2} \quad (3.19)$$

This last expression is an explicit form of $E_{AQ,EDi}$ in eq 3.13. The average square fluctuations away from equilibrium $\langle\delta q^2\rangle_L$ and $\langle\delta Q^2\rangle_{cl}$ in eqs 3.18 and 3.19 arise due to the connection of a_L eq 2.10 to the quantum average square fluctuation of the proton coordinate

$$a_L = m\omega_L/\hbar = {}^1/_2\langle\delta q^2\rangle_L \quad (3.20)$$

and b to the thermal classical average square fluctuation of Q

$$b_o = m_Q\omega_Q{}^2/RT_o = 1/\langle\delta Q^2\rangle_{cl} \quad (3.21)$$

(Note that from the relation between X and Q, $X = Q - r_{AHeq} - r_{HBeq}$, the thermal average square fluctuation of Q is equivalent to the thermal average square fluctuation of X: $\langle\delta X^2\rangle = \langle\delta Q^2\rangle$.) The expression for the overlap in eq 3.18 is what one would expect for the overlap of two harmonic oscillator (HO) wave functions, i.e., overlap of two Gaussians, with an exponential argument that is the square of separation of the two HO potentials divided by total average square fluctuations along the respective overlap coordinate. Since there are two wells, one gets quantum fluctuations from each R and P well

$$a_L = 1/(\langle\delta q^2\rangle_L{}^R + \langle\delta q^2\rangle_L{}^P) \quad (3.22)$$

By comparing eqs 3.16 and 3.19, one can define an inverse length parameter α_{EDiL} comparable to α_{EAdL} of EAd PT

$$\alpha_{EDiL} = (1/2)X_{eq}/(\langle\delta Q^2\rangle_{cl} + 2\langle\delta q^2\rangle_L) \quad (3.23)$$

For systems i and ii, $\alpha_{EAdH} = 29$ Å^{-1} and $\alpha_{EAdD} = 41$ Å^{-1}, while eq 3.23 gives $\alpha_{EDiH} = 29.9$ Å^{-1} and $\alpha_{EDiD} = 37.5$ Å^{-1}. The numerical similarity, for individual isotopes, of the αs numerically explains why the $E_{AQ,L}$s are of the same order of magnitude in Tables 2 and 3. However, the isotope difference in αs is distinct: $\alpha_{EAdD} = \sqrt{2}\alpha_{EAdH}$, while $\alpha_{EDiD} = 1.254\alpha_{EDiH}$. Hence, the larger isotope difference in αs for EAd PT gives the larger difference $E_{AQ,D} - E_{AQ,H}$. The origin of this isotope difference in αs for EDi PT is now discussed.

The isotope dependence of $\alpha_{EAdL} \propto \sqrt{m_L}$ for EAd PT arises from the coupling between the proton wavefunction overlap derived from electronically adiabatic proton potentials, and the H-bond coordinate Q, i.e., the Q dependence of C in eq 3.5.[2] For EDi PT, this coupling α_{EDiL} is derived from an overlap dependence on Q, derived from electronically diabatic proton potentials, and as such depends on the average square fluctuation of the H-bond and proton modes along the tunneling coordinate, cf. eq 3.23. The isotope dependence of α_{EDiL} is contained solely in $\langle\delta q^2\rangle_L = 1/\sqrt{m_L}$. If $\langle\delta Q^2\rangle_{cl} \ll \langle\delta q^2\rangle_L$, the isotope dependence of eq 3.23 will be $\alpha_{EDi,L} \propto \sqrt{m_L}$, identical to that of the adiabatic PT counterpart α_{EAdL}. In the opposite limit $\langle\delta Q^2\rangle_{cl} \gg \langle\delta q^2\rangle_L$, which corresponds to an extremely classical Q mode, α_{EDiL} is isotope-independent resulting in an extremely small difference $E_{AQ,D} - E_{AQ,H}$. For systems i and ii, the two averages $\langle\delta Q^2\rangle_{cl}$ and $\langle\delta q^2\rangle_L$ are similar in magnitude, and thus the difference $E_{AQ,D} - E_{AQ,H}$ for EDi PT is smaller than that for EAd PT in the classical Q mode description.[33]

4. Concluding Remarks

Here we have compared the proton transfer (PT) rate constants and KIEs for electronically adiabatic (EAd) and electronically diabatic (EDi) perspectives. The drastic difference in the treatment of the electronic character of the PT in the two perspectives produces significant differences in rate constants and KIEs, with smaller rate constant magnitudes and larger KIEs with a smaller variation with reaction asymmetry, and a smaller activation energy difference $E_{AD} - E_{AH}$ than does the EAd PT treatment. The basic origin of these features is that the "nonadiabatic coupling" element which is associated with the tunneling probability via the overlap of proton wave functions for EDi PT is smaller and less sensitive to both H-bond motion and proton excitation than those for EAd PT, and the contribution from excited L states is larger for EAd PT than for EDi PT.

We reiterate that the EDi PT perspective requires weak electronic coupling between the proton donor and acceptor states. In the model calculations presented within, the electronic resonance coupling is ~−19 kcal/mol, which is the appropriate magnitude for PT within an H-bonded complex. An EDi PT perspective can only be physically valid with an electronic coupling much less than 1 kcal/mol,[16,17] but for normal proton, H atom, and hydride transfers, the electronic coupling is expected to be far larger than such small values.[8,11,16,17,18,34]

Acknowledgment. This work was supported in part by NSF Grants CHE-9700419, CHE-0108314, and CHE-0417570 and the Cristol Fund from the Department of Chemistry and Biochemistry at the University of Colorado at Boulder.

References and Notes

(1) Kiefer, P. M.; Hynes, J. T. *J. Phys. Chem. A* **2004**, *108*, 0000.

(2) (a) Borgis, D.; Hynes, J. T. *J. Phys. Chem.* **1996**, *100*, 1118. (b) Borgis, D.; Hynes, J. T. *Chem. Phys.* **1993**, *170*, 315. (c) Borgis, D.; Lee, S.; Hynes, J. T. *Chem. Phys. Lett.* **1989**, *162*, 19. (d) Borgis, D.; Hynes, J. T. *J. Chem. Phys.* **1991**, *94*, 3619. (e) Lee, S.; Hynes, J. T. *J. Chim. Phys.* **1996**, *93*, 1783.

(3) (a) Cha, Y.; Murray, C. J.; Klinman, J. P. *Science* **1989**, *243*, 1325.-(b) Kohen, A.; Klinman, J. P. *Acc. Chem. Res.* **1998**, *31*, 397. (c) Kohen, A.; Klinman, J. P. *Chem. Biol.* **1999**, *6*, R191. (d) Kohen, A.; Cannio, R.; Bartolucci, S.; Klinman, J. P. *Nature (London)* **1999**, *399*, 496.

(4) (a) Rickart, K. W.; Klinman, J. P. *Biochemistry* **1999**, *38*, 12218. (b) Knapp, M. J.; Rickart, K. W.; Klinman, J. P. *J. Am. Chem. Soc.* **2002**, *124*, 3865.

(5) (a) Basran, J.; Sutcliffe, M. J.; Scrutton, N. S. *Biochemistry* **1999**, *38*, 3218. (b) Harris, R. J.; Meskys, R.; Sutcliffe, M. J.; Scrutton, N. S. *Biochemistry* **2000**, *39*, 1189. (c) Basran, J.; Patel, S.; Sutcliffe, M. J.; Scrutton, N. S. *J. Biol. Chem.* **2001**, *38*, 3218.

(6) (a) Basner, J. E.; Schwartz, S. D. *J. Phys. Chem. B* **2004**, *108*, 444. (b) Antoniou, D.; Schwartz, S. D. *Proc. Natl. Acad. Sci. U.S.A.* **1997**, *94*, 12360. (c) Antoniou, D.; Schwartz, S. D. *J. Chem. Phys.* **1999**, *110*, 465. (d) Karmacharya, R.; Schwartz, S. D. *J. Chem. Phys.* **1999**, *110*, 7376.

(7) (a) Brunton, G.; Griller, D.; Barclay, L. R. C.; Ingold, K. U. *J. Am. Chem. Soc.* **1976**, *98*, 6803. (b) Brunton, G.; Gray, J. A.; Griller, D. Barclay, L. R. C.; Ingold, K. U. *J. Am. Chem. Soc.* **1978**, *100*, 4197.

(8) (a) Agarwal, P. K.; Billeter, S. R.; Hammes-Schiffer, S. *J. Phys. Chem. B* **2002**, *106*, 3283. (b) Agarwal, P. K.; Billeter, S. R.; Rajagopalan, P. T.; Benkovic, S. J.; Hammes-Schiffer, *Proc. Natl. Acad. Sci. U.S.A.* **2002**, *99*, 2794. (c) Hammes-Schiffer, S. *Chem. Phys. Chem.* **2002**, *3*, 33. (d) Hammes-Schiffer, S.; Billeter, S. R. *Int. Rev. Phys. Chem.* **2001**, *20*, 591. (e) Billeter, S. R.; Webb, S. P.; Agarwal, P. K.; Iordanov, T.; Hammes-Schiffer, S. *J. Am. Chem. Soc.* **2001**, *123*, 11262. (f) Billeter, S. R.; Webb, S. P.; Iordanov, T.; Agarwal, P. K.; Hammes-Schiffer, S. *J. Chem. Phys.* **2001**, *114*, 6925. (g) Hammes-Schiffer, S. *Curr. Opin. Struct. Biol.* **2004**, *14*, 192.

(9) (a) Dogonadze, R. R.; Kuznetzov, A. M.; Levich, V. G. *Electrochim. Acta* **1968**, *13*, 1025. (b) German, E. D.; Kuznetzov, A. M.; Dogonadze, R. R. *J. Chem. Soc., Faraday Trans. 2* **1980**, *76*, 1128. (c) Kuznetzov, A. M. *Charge Transfer in Physics, Chemistry and Biology: Physical Mechanisms of Elementary Processes and an Introduction to the Theory*; Gordon and Breach Publishers: Amsterdam, 1995. (d) Kuznetzov, A. M.; Ulstrup, J. *Can. J. Chem.* **1999**, *77*, 1085. (e) Sühnel, J.; Gustav, K. *Chem. Phys.* **1984**, *87*, 179.

(10) Siebrand, W.; Wildman, T. A.; Zgierski, M. Z. *J. Am. Chem. Soc.* **1984**, *106*, 4083, 4089.

(11) (a) Cukier, R. I. *J. Phys. Chem. B*, **2002**, *106*, 1746. (b) Cukier, R. I.; Zhu, J. *J. Phys. Chem. B* **1997**, *101*, 7180.

(12) (a) Ando, K.; Hynes, J. T. *J. Phys. Chem. B* **1997**, *101*, 10464. (b) Ando, K.; Hynes, J. T. *J. Phys. Chem. A* **1999**, *103*, 10398. (c) Staib, A.; Borgis, D.; Hynes, J. T. *J. Chem. Phys.* **1995**, *102*, 2487. (d) Ando, K.; Hynes, J. T, *Adv. Chem. Phys.* **1999**,*110*, 381. (e) Ando, K.; Hynes, J. T. *J. Mol. Liq.* **1995**, *64*, 25.

(13) The description of PT in previous work[12, 14] has its foundation in the Mulliken charge-transfer picture for PT (cf. ref 33 in ref 14a), in which an electron is transferred from a nonbonding orbital on the base to the antibonding orbital of the acid, a picture supported via ab initio calculations in ref 12, parts a and b. If one thought in weak electronic coupling terms, an H atom would then be transferred. Of course, the electron coupling is very large, such that this view of a separate electron transfer followed by an H atom transfer is incorrect; instead the electron and H atom transfer are concerted.[12.]

(14) (a) Kiefer, P. M.; Hynes, J. T. *J. Phys. Chem. A* **2002**,*106*, 1834. (b) Kiefer, P. M.; Hynes, J. T. *J. Phys. Chem. A* **2002**,*106*, 1850.

(15) These remarks apply to the ground electronic state. They would not apply for example in an excited electronic state in the neighborhood of a conical intersection involving the proton coordinate; see, e.g.: Granucci, G.; Hynes, J. T.; Millíe, P.; Tran-Thi, T.-H. *J. Am. Chem. Soc.* **2000**, *122*, 12235.

(16) (a) Cukier, R. I. *J. Phys. Chem.* **1996**, *100*, 15428. (b) Cukier, R. I.; Nocera, D. *Annu. Rev. Phys. Chem.* **1998**, *49*, 337.

(17) (a) Soudackov, A.; Hammes-Schiffer, S. *J. Chem. Phys.* **2000** *113*, 2385. (b) Iordanova, N.; Decornez, H.; Hammes-Schiffer, S. *J. Am. Chem. Soc.* **2001**, *123*, 3723. (c) Iordanova, N.; Hammes-Schiffer, S. *J. Am. Chem. Soc.* **2002**, *124*, 4848.

(18) (a) Hammes-Schiffer, S. *Acc. Chem. Res.* **2001**, *34*, 273. (b) Hammes-Schiffer, S.; Iordanova, N. *Biochim. Biophys. Acta* **2004**, *1655*, 29.

(19) The electronic resonance coupling is qualitatively described by the overlap between two e*lectronic* diabatic state wave functions, while the proton coupling is described by the overlap between two *nuclear* diabatic proton wave functions. The reorganization energy for ET is defined in a electronically diabatic perspective, and is defined[20] by a relaxation free energy difference, from a product electronic diabatic state—reached in a Franck−Condon electronic excitation from the equilibrium reactant solvent position on the reactant electronic diabatic surface—to the equilibrium product solvent position.

(20) (a) Marcus, R. A. *J. Chem. Phys.* **1956**, *24*, 966; 979. (b) Marcus, R. A.; Sutin, N. *Biochim. Biophys. Acta* **1985**, *811*, 265. (c) Sutin, N. *Prog. Inorg. Chem.* **1983**, *30*, 144.

(21) X_{eq} is equivalent to ΔX in ref 9.

(22) This is the first place where a quantum average over the H-bond mode could be usefully introduced in generalizing the EDi PT perspective. In particular, the overlap $S_{n_R n_P}$ could instead include the overlap of two-dimensional wave functions, one for the proton and one for the H-bond mode. This would be similar to that of eq 2.11 of paper 1,[1] and it would specifically include a reorganization energy for the H-bond mode. However, we do not carry out this generalization but continue to employ the EDi PT description currently used to analyze tunneling PT data.

(23) Timoneda, J. J.; Hynes, J. T. *J. Phys. Chem.* **1991**, *95*, 10431.

(24) Thompson, W. H.; Hynes, J. T. *J. Phys. Chem. A* **2001**, *105*, 2582.

(25) The coefficients $c_{in_R n_P}$ in eq 2.7 are readily derived from eq 2.4. For example, $c_{000} = 1$, $c_{010} = c_{001} = 0$, $c_{110} = c_{101} = 1$, $c_{011} = 1$, $c_{111} = -2$, and $c_{211} = 1$.

(26) The integral in eq 2.12 is a sum of integrals of the form

$$\int_{-\infty}^{\infty} dY\,(Y+B)^{2i} e^{-(a_L+b)/2\,Y^2} = \sum_{n=0}^{i} f_n(B) I_n;$$

$$I_n = \int_{-\infty}^{\infty} dY\,(Y)^{2n} e^{-(a_L+b)/2\,Y^2}$$

where

$$I_n = \frac{1\cdot 3\cdot 5 \ldots (2n-1)}{(a_L+b)^n}\sqrt{\frac{2\pi}{a_L+b}}$$

(cf. Gradstein, I. S.; Ryzhik, I. M. *Table of Integrals, Series and Products*; Academic Press: New York, 1980). This defines γ_i in eq. 2.13 as

$$\gamma_i = \sum_{n=0}^{i} f_n(B)\,\frac{1\cdot 3\cdot 5 \ldots (2n-1)}{(a_L+b)^n}$$

(27) Kiefer, P. M.; Hynes, J. T. *J. Phys. Chem. A* **2003**, *107*, 9022.

(28) The following parameters ($\epsilon_o = 80$ and $M_S = 0.7$, with $\mu_P - \mu_R = 8$ D for i and $\mu_P - \mu_R = 6$ D for ii) were chosen to obtain these values of E_S. M_S is a factor dependent on the structure of the H-bond complex.[14,23,27]

(29) Kiefer, P. M.; Hynes, J. T. *Isr. J. Chem.* **2004**, *44*, 171.

(30) The literature concerning this solvent coordinate for both PT and ET is quite extensive (for examples, see ref 14). For the present model system, ΔE is the energetic offset between the electronically diabatic states, which is modulated by the nonequilibrium solvation of the surrounding dielectric continuum[14,29] $\Delta E = -\Delta_{vac} - K(\mu_R - \mu_P)z - (1/2)K_\infty(\mu_R^2 - \mu_P^2)$, where Δ_{vac} is the gas-phase offset between the reactant and product VB states, and K_∞ is the force constant for the electronic polarization of the solvent $K_\infty = 2M_S(1 - 1/\epsilon_\infty)$, $\epsilon_\infty = 2$. z describes the orientational polarization of the solvent configuration and corresponds to the solute dipole moment that the solvent configuration would be equilibrated to *if* there were equilibrium solvation, which in general there is not.

(31) Note that the KIE vs ΔG_{RXN} behavior in Figure 3 for the 0−0 transition is not maximal for the symmetric reaction, $\Delta G_{RXN} = 0$. For the total rate constant given by eqs 2.17 and 2.18 in paper 1,[1] the maximum indeed occurs exactly at $\Delta G_{RXN} = 0$. In this paper, we however use the approximate form eqs 2.24 and 2.25 of paper 1.[1] With this approximate

form, the moderate to high T regime ($\hbar\omega_Q/RT \sim 1$ and $\hbar\omega_Q/RT < 1$) has a reaction barrier vs reaction asymmetry dependence that is isotope-dependent, eq 3.3. For example, for the 0−0 rate given by eq 3.2, the isotope-dependent eq 3.3 defines the maximum in a KIE vs reaction asymmetry plot that is shifted away from $\Delta G_{RXN} = 0$ of, i.e., the reaction asymmetry ΔG_{RXN}^{max} that minimizes the difference $\Delta G_D^{\ddagger} - \Delta G_H^{\ddagger}$, which is the shift $\Delta G_{RXN}^{max} = -E_S(\gamma - 1)/\gamma$, where $\gamma = (\beta\hbar\omega/2)\coth(\beta\hbar\omega/2)$, which is always greater than 1 such that the maximum has $\Delta G_{RXN}^{max} < 0$. The addition of the ΔG_{RXN} behavior from excited-state transition rates for the total rate constant shifts the maximum near $\Delta G_{RXN} = 0$.

(32) In general, the thermal average of the square proton coupling over H-bond motion is[2] $\langle C_L^2\rangle = C_{eq,L}^2 \exp(2\alpha_L^2\langle\delta Q^2\rangle)$, where $\langle\delta Q^2\rangle$ is not exclusively classical. From eq 3.15, the expression for $E_{AQL,EAd}$ is $E_{AQL} = -2\alpha_L^2\partial\langle\delta Q^2\rangle/\partial(1/RT)|_{T=T_o}$, such that the resulting form is given by eq 3.11. The EDi PT formalism has been cast solely in the classical H-bond mode limit, and thus, the only limit with which one can compare E_{AQL}s. See ref 22 for a possible extension of EDi PT to include a nonclassical H-bond mode.

(33) The ratio $\langle\delta Q^2\rangle_{cl}/\langle\delta q^2\rangle_L$ describes the relative fluctuations of the classical H-bond and quantum proton modes, becoming smaller as the H-bond mode frequency decreases, i.e. $\hbar\omega_Q \ll RT$ and the classical Q description becomes more appropriate. For example, consider a smaller H-bond frequency $\hbar\omega_Q = 100\ cm^{-1}$ instead of $\hbar\omega_Q = 300\ cm^{-1}$ (for which the quantum treatment by EAd PT is more appropriate) for i and ii. This 3-fold decrease in $\hbar\omega_Q$ results in a 9-fold increase in $\langle\delta Q^2\rangle_{cl}$ and makes the isotope dependence in eq 3.23 and the difference $E_{AQ,D} - E_{AQ,H}$ much less than for the 300 cm^{-1} case: $\alpha_{EDiH} = 8.6\ Å^{-1}$ and $\alpha_{EDiD} = 9.1\ Å^{-1}$.

(34) (a) Warshel, A. *Acc. Chem. Res.* **2002**, *35*, 385. (b) Warshel, A.; Parson, W. W. *Q. Rev. Biophys.* **2001**, *34*, 563. (c) Villa, J.; Warshel, A. *J. Phys. Chem. B* **2001**,*105*, 7887.